95-28

Environment Canada
Water Science and Technology Directorate

Direction générale des sciences et de la technologie, eau
Environnement Canada

Automated analysis of hydraulic and tracer Tests conducted in fractured rock

By:
A. Piggott, T. Huynh, P. Lapcevic, K. Novakowski

95-28

Management Perspective

Hydraulic and tracer tests are frequently used to determine the properties of a geologic formation that regulate the processes of groundwater flow and contaminant transport. These tests involve the injection, or withdrawal, of fluid at a source well and the monitoring of groundwater levels or tracer concentration at one or more observation wells. The properties that are determined from the test results are often obtained by matching the recorded data to type-curves derived by mathematical approximation of fluid flow and tracer transport. Manual comparison of the data to type-curves is frequently used to obtain the match but is an onerous task that yields only a qualitative result. A method of automated type-curve matching is developed using an existing library of approximations for fluid flow and tracer transport. This approach reduces the effort associated with the analysis, eliminates much of the subjectivity of manual interpretation, and provides a statistically optimal representation of the measured data. The performance of the procedure relative to conventional, manual methods of type-curve matching is demonstrated through application to data collected during in situ characterization of groundwater flow and transport within fractured rock.

Automated Analysis of Hydraulic and Tracer Tests Conducted in Fractured Rock

Andrew R. Piggott, Theresa N.T. Huynh, Pat A. Lapcevic and Kent S. Novakowski

National Water Research Institute
867 Lakeshore Road
Burlington, Ontario L7R 4A6, Canada
(905) 336-6245 and FAX (905) 336-4400
Andrew.Piggott@CCIW.Ca

NWRI Contribution 95-28

June 1995

Abstract

An algorithm is presented for automated type-curve matching of hydraulic and tracer test data. The algorithm determines formation parameters by linking existing models of fluid flow and tracer transport in fractured rock to a robust, nonlinear regression routine. This method of parameter determination reduces the effort and subjectivity associated with manual interpretation of the data and returns an optimal representation of the data. Application of the algorithm to a range of hydraulic and tracer test data demonstrates the advantages of the approach relative to conventional methods of type-curve matching.

Introduction

Hydraulic and tracer tests are frequently used to determine the hydrogeological properties of a formation. Hydraulic tests include both pulse and pumping formats. In pulse tests, a finite volume of fluid is injected into the formation at a source well and the variation of hydraulic head at an observation well is monitored. In pumping tests, fluid is withdrawn from the source well at a constant rate, again with monitoring of hydraulic head at the observation well; a recovery period during which hydraulic head returns to ambient levels may follow the period of fluid withdrawal. Tracer tests involve the injection of fluid at a source well where a finite volume of the fluid is tagged with a solute tracer. The breakthrough of the tracer at an observation well is determined by monitoring the variation of tracer concentration.

Formation properties are often obtained from hydraulic and tracer test results by matching the measured data to type-curves derived by mathematical approximation of fluid flow and tracer transport. Type-curves are available for various in situ conditions and represent hydraulic head or tracer concentration as a function of time and the relevant formation parameters. Manual comparison of the measured data to type-curves is a common method of obtaining the match but is an onerous task that yields only a qualitative result. Automated type-curve matching is a form of inverse analysis where the formation parameters are determined using the mathematical models that form the type-curves in conjunction with methods of nonlinear regression. This computer-assisted approach is particularly well developed within petroleum reservoir engineering and is recognized as offering several advantages relative to manual methods of analysis (Earlougher, 1977; Horne, 1990). Specifically, type-curve matching by inverse analysis reduces the effort associated with the interpretation of data, eliminates much of the subjectivity of the interpretation, and provides a statistically optimal representation of the measured data.

This paper describes an inverse analysis capability for the TYPCURV and RADT models of hydraulic and tracer tests conducted in fractured rock. The TYPCURV algorithm is described in Novakowski (1990) and includes Laplace transform solutions for the hydraulic head induced by pulse and pumping tests where the results are influenced by wellbore storage and skin effects. RADT is a model of tracer transport that implements the analytical solutions reported in Novakowski (1992). This model includes Laplace transform solutions for tracer breakthrough where the results are influenced by wellbore mixing and matrix diffusion. While TYPCURV and RADT were developed specifically for flow and transport in fractured rock, the solutions are equally valid for porous formations and therefore the resulting inverse analysis algorithm is applicable to a useful range of in situ conditions.

Formulation of an Inverse Analysis Capacity for TYPCURV and RADT

The approach that was applied in the formulation of an inverse analysis capacity for TYPCURV and RADT parallels the approach applied by Piggott et al. (1994) in developing an inverse analysis implementation of the SUTRA model of groundwater flow and transport (Voss, 1984). The following outlines this approach; additional details regarding the procedure are presented in Piggott et al. (1994).

Both TYPCURV and RADT return dimensionless results in anticipation of interpretation using conventional methods of type-curve matching. In this application, the dimensionless hydraulic heads returned by TYPCURV, h_d, are translated into dimensional values, h, using

$$h = h_o + \Delta h \, h_d \tag{1}$$

for pulse tests and

$$h = h_o + \frac{Q}{2 \pi T} h_d \tag{2}$$

for pumping tests. Here, h_o is the ambient hydraulic head in the formation, Δh is the hydraulic head applied at the source well in a pulse test, and Q and T are the pumping rate and transmissivity in a pumping test. Similarly, RADT returns dimensionless tracer concentrations, c_d, that are transformed into dimensional quantities, c, using

$$c = c_o + \Delta c \, c_d \tag{3}$$

where c_o is the ambient concentration of the tracer in the formation and Δc is the concentration of the tracer that is injected at the source well.

Conducting a hydraulic or tracer test, and measuring hydraulic head or tracer concentration in an observation well, may be represented symbolically as

$$\underline{h}_m = F_m(\underline{p}_m) \tag{4}$$

where $\underline{h}_m$ is a vector that contains the observations of hydraulic head or tracer concentration, $\underline{p}_m$ is a vector that contains the parameters that describe the formation (transmissivity, porosity, etc.), and F_m represents the translation of the parameters into the measured data.

Numerical determination of hydraulic heads or tracer concentrations using TYPCURV or RADT may be expressed in the analogous form

$$\underline{h}_c = F_c(\underline{p}_c) \tag{5}$$

where $\underline{h}_c$ contains the calculated results, $\underline{p}_c$ contains the input values of the formation parameters, and F_c represents the translation of the parameters into the calculated results. If TYPCURV and RADT are configured such that the times at which the measured and calculated quantities are defined are coincident, then the measured data and calculated results can be compared to determine the accuracy of the input parameters in Equation (5) as an estimate of the formation parameters in Equation (4).

Formally stated, inversion of the measured data to yield the formation parameters is represented by the symbolic relation

$$\underline{p}_m = F_c^{-1}(\underline{h}_m) \ . \tag{6}$$

In practice, the parameter estimates derived by inversion of the measured data differ from the in situ values due to measurement errors entrained in the data, and the failure of the models to fully represent in situ conditions. For example, TYPCURV and RADT assume homogeneous and isotropic conditions, an assumption that may be unrealistic in many in situ settings.

Equation (6) expresses inversion of the measured data in a symbolic manner. In application, inversion is accomplished using an iterative procedure in which an estimate of the formation parameters is submitted to TYPCURV or RADT, the output calculated results are compared to the measured data, and a revised estimate of the parameters is derived from the results of the comparison. An optimization algorithm is used to automate the process of identifying the formation parameter values that correspond to the minimum discrepancy between the measured data and calculated results.

Parameter Relations

The calculated results returned by TYPCURV and RADT are regulated by numerous input parameters. Here, these are referred to as physical parameters since the parameters have a physical implication (they represent transmissivity, porosity, etc.). Typically, only a few of the physical parameters are determined by type-curve matching, and an initial estimate and a permissible range of values for each of the parameters are available prior to the analysis. Accommodating this information requires a sequence of parameter transformations that replace the physical parameters with optimization parameters.

It is convenient to define a vector of scaled parameters, $\underline{q}$, by normalizing the physical parameters with respect to the permissible range of values assigned to the parameters. The relation between the scaled and physical parameters may be stated as

$$\underline{p} = \underline{p}_{min} + \underline{T}_q \underline{q} \tag{7}$$

where $\underline{T}_q$ is a transformation matrix that implements scaling between the prescribed minimum and maximum values of the physical parameters, $\underline{p}_{min}$ and $\underline{p}_{max}$.

The scaled parameters are determined from the optimization parameters, $\underline{r}$, using

$$\underline{q} = \underline{q}_{est} + \underline{T}_r \underline{r} \tag{8}$$

where $\underline{T}_r$ is a second transformation matrix and

$$\underline{q}_{est} = \underline{T}_q^{-1} (\underline{p}_{est} - \underline{p}_{min}) \tag{9}$$

with $\underline{p}_{est}$ defined as an initial estimate of the physical parameters. Formulating the transformation matrix in Equation (8) is an exercise in bookkeeping. Three constraint conditions can be achieved: 1) parameter values can be maintained at the specified input values, 2) parameter values can be independently variable, and 3) parameter values can be variable yet constrained to be equal to any other parameter value. The latter condition can be used, for example, to determine the storativity of the unaltered and near-wellbore regions of a formation such that the values remain equal throughout the analysis.

Definition of the Error Function

An error function is required as a quantitative metric of the discrepancy between the measured data and the calculated results corresponding to an estimate of the optimization parameters. The least absolute value criterion is one suitable form of the error function (Rosa and Horne, 1991; Xiang et al., 1993)

$$E(\underline{r}) = \frac{1}{\sum_i w_i} \sum_i w_i \, |h_{c,i} - h_{m,i}| \qquad (10)$$

where $h_{c,i}$ and $h_{m,i}$ are the entries of the vectors of calculated results and measured data and w_i are entries of a vector of weighting factors.

The weighting factors are defined such that the error function is averaged over the duration of the observations. If the data points are to be uniformly weighted, then the weighting factors are simply

$$w_i = \frac{1}{N_m} \, . \qquad (11)$$

Alternatively, the weighting factors are defined as

$$w_i = \frac{t_{m,i+1} - t_{m,i-1}}{2} \qquad (12)$$

if time is to be represented on a linear scale. Finally, the weighting factors are defined as

$$w_i = \frac{\log t_{m,i+1} - \log t_{m,i-1}}{2} \qquad (13)$$

if time is to be represented on a logarithmic-linear scale. The latter alternative is equivalent to type-curve matching with time expressed on a logarithmic axis. Parameter estimates based on weighting factors computed using Equations (11), (12), and (13) differ as an improved match is sought for data that are assigned larger weighting factors. For example, weighting the deviations in a logarithmic-linear manner emphasises data collected at small values of time to relative to data collected at large values of time.

The prescribed permissible range of values of the physical parameters is enforced using a penalty approach in which a large, penalty value is assigned to the error function whenever an estimate of the optimization parameters violates the constraints. The optimization algorithm interprets this as a very poor approximation of the measured data and therefore this procedure prohibits the selection of optimization parameter values that violate the prescribed constraints.

Minimization of the Error Function

The best estimate of the optimization parameters is determined by minimizing the error function with respect to each of the parameters. This is equivalent to nonlinear regression and is achieved using an optimization algorithm that systematically adjusts the parameters such that the algorithm terminates at the minimum value of the error function.

Many methods of multivariate optimization have been reported in the literature and numerous of these approaches are suitable for application to the problem at hand. Previous experience (Piggott et al., 1992; Piggott and Elsworth, 1993; Piggott et al., 1994) has demonstrated that the polytope optimization algorithm described by Nelder and Mead (1965) and implemented in Press et al. (1992) is a reliable approach when subject to the termination criteria of Gioda and Maier (1980). This method is highly robust and is well suited to this application as it does not require the evaluation of derivative information and is less sensitive to the spurious behaviour that is occasionally noted for TYPCURV and RADT (Carroll and Horne, 1992).

Implementation of the Inverse Analysis Algorithm

The inverse analysis algorithm outlined in this paper has been implemented as FORTRAN source code. Copies of the program, TCINV (type-curve matching by inverse analysis), may be obtained by contacting the senior author or via the Internet at http://gwrp.cciw.ca or ftp://gwrp.cciw.ca. Guidelines for the use of TCINV, including input and output file specifications, are detailed in Piggott (1995).

Minimal revisions to the source codes for TYPCURV and RADT were required in the preparation of TCINV. The majority of the revisions were required to convert the algorithms from stand-alone programs to subroutines referenced by TCINV, and to direct input and output to and from TCINV. Verification studies indicate that the full range of functionalities of TYPCURV and RADT are available in inverse analysis.

Extensive use of RADT has revealed that the program is subject to failure at small and large values of time, a behaviour that is exhibited by many methods of numerical simulation of solute transport. Solution criteria that predict the failure of RADT as a function of the input parameters are reported in Piggott and Novakowski (1995) and have been implemented in TCINV. Enforcing these stability criteria prevents the premature termination analyses due to the failure of RADT.

TCINV includes various facilities that assist analysis. These include facilities for forming the parameter transformation matrices, computing the weighting functions, initializing the optimization algorithm, determining the penalty value of the error function, and adjusting the weighting factors to accommodate calculated results that are not accessible subject to the solution criteria applied to RADT. Finally, the modular structure of TCINV facilitates the integration of models of groundwater flow and transport, making TCINV useful as a generalized scheme for the inverse analysis of aquifer test results.

Example Analyses

The following analyses demonstrate the application of TCINV to data derived from a detailed, in situ investigation of groundwater flow and transport within a single fracture in rock. The site where this study is being performed is situated near Toronto, Canada and consists of an array of 25 boreholes that intersect a single horizontal fracture. The fracture is located approximately 10.5 m below the ground surface and is associated with a limestone interbed in Ordovician aged shale. A range of hydraulic and tracer tests have been conducted at the site. Thorough descriptions of the geological setting and experimental protocols associated with this study are reported in Novakowski (1988) and Novakowski and Lapcevic (1994).

Analysis of Pulse Test Data

The first example involves the analysis of the results of a hydraulic test. The test was conducted by instantaneously introducing a volume of water into the source well and observing the variation of hydraulic head in an observation well located 14.9 m from the source well. Open wellbore conditions were maintained in the source well with a known wellbore storage factor; packers were used to maintain near shut-in conditions in the observation well. Figure 1 illustrates the measured data collected during the test and compares the data to a range of calculated results. Here, the points indicate the measured data, the dashed line indicates the results obtained by manual type-curve matching, and the solid lines indicate the results obtained by inverse analyses with various modelling assumptions. Specifically, Case 1 corresponds to the determination of the transmissivity and storativity of the formation, T_2 and S_2, assuming no skin effects while Cases 2 and 3 correspond to the determination of transmissivity and storativity assuming infinitesimal and finite thickness skin, respectively. Table 1 summarizes the parameter values extracted from the measured data and lists the residual values of the error function obtained from the analyses.

Consistently, the calculated results obtained by inverse analysis better approximate the measured data than the results obtained by manual type-curve matching. This is apparent both qualitatively in Figure 1 and quantitatively in Table 1. Assuming infinitesimal and finite thickness skin (Cases 2 and 3) results in a similar approximation of the measured data, with both results providing an improved match relative to the assumption of no skin effects (Case 1). Cases 2 and 3 return similar estimates of the transmissivity and storativity of the fracture and the parameters that regulate the skin effect (the skin factor, S_{k2}, for infinitesimally thin skin and the radius, r_s, transmissivity, T_1, and storativity, S_1 of the skin region for finite thickness skin) consistently indicate a near-wellbore region of reduced transmissivity. The parameters that regulate the skin effect in Case 3 are not unique; that is, various sets of values return an identical approximation due to the manner in which these parameters form the skin effect. In Case 3, the storativity of the skin is constrained as equal to the storativity of the unaltered portion of the formation in order to reduce the number of degrees of freedom in the analysis. This is not a necessary assumption, but is justified given the non-unique nature of the outcome.

Analysis of Pumping Test Data

Figure 2 compares the measured data and calculated results obtained for a pumping test performed between the source and observation wells described previously. In this test, water was withdrawn from the source well at a rate of 6.1×10^{-6} m^3/s for 3.83×10^3 s with the duration of pumping followed by an equivalent duration of recovery. Table 2 lists the parameter values corresponding to the results shown in Figure 2. In this analysis, Case 1 indicates the determination of the transmissivity and storativity of the fracture subject to the assumption of no skin effects and Cases 2, 3, and 4 indicate the assumption of infinitesimal thickness skin in the source well, finite thickness skin in the source well, and infinitesimal thickness skin in both the source and observation wells, respectively. Again, the results for Case 3 are non-unique and the storativity of the skin region is constrained as equal to the storativity of the unaltered portion of the formation. The results obtained for Cases 1 through 4 are very similar with only a slight difference in the match obtained at the onset of pumping and recovery. This suggests that skin effects have a minimal influence on the test results, a conclusion that is supported by the similarity of the transmissivity and storativity estimates derived without (Case 1) and with (Cases 2, 3, and 4) skin effects. In contrast to the pulse test, the parameters that regulate the source well skin effect (S_{k2} and r_s, T_1, and S_1) consistently indicate a region of elevated transmissivity in the vicinity of the source well. Reduced transmissivity in the vicinity of the observation well is evidenced by the computed value of the skin factor for the observation well (S_{k1}). Again, there is a significant difference between the values of the transmissivity and storativity of the fracture derived by manual type-curve matching and inverse analysis.

Analysis of Tracer Test Results

The third set of results were derived from a radial divergent tracer test performed between a source well and an observation well located 26.6 m from the source well. This test was performed on the same fracture as the pulse and pumping tests but involved different source and observation wells. The test was conducted by injecting water into the fracture at a rate of 1.2×10^{-5} m^3/s and tagging a volume of the injected water with a tracer of known concentration. A mixing apparatus was installed in the source well to ensure predictable mixing of the tracer and resident water and a specially designed packer was used to minimize the volume of the observation well where sampling for tracer concentration was performed.

Figure 3 compares the measured data derived from the tracer test to the results obtained by manual type-curve matching and inverse analysis of the data. Tracer concentration is depicted in normalized form, relative to the input concentration. Here, Case 1 indicates the determination of fracture aperture, b, dispersivity, α_r, and matrix porosity, θ_2, from the data. Case 2 extends this analysis to include the tortuosity of flow within the fracture by adjusting the distance between the source and observation wells, r_i. Table 3 lists the parameter values determined from the analyses.

As in the previous analyses, the inverse analysis results better approximate the measured data than the results obtained by manual type-curve matching. Similarly, the results obtained for Case 2 better approximate the measured data than the results obtained for Case 1 with the distance between the source and observation wells determined in Case 2 appearing as less than the physical distance. This may indicate channelling, wherein preferential tracer transport occurs within regions of elevated conductivity.

Discussion and Conclusions

Determination of the hydrogeologic properties of a formation by the inverse analysis of hydraulic and tracer test data improves on the interpretation of the data by manual type-curve matching. The advantages of the automated approach include a reduction in the effort and subjectivity associated with the analysis, and the identification of the optimal match between the measured data and calculated results and therefore the best estimates of the properties. These advantages are amply demonstrated in the preceding analyses. The manual type-curve matching results cited in this paper were developed by an experienced practitioner; therefore, the results of the automated and manual approaches are an accurate indication of the relative performance of the approaches, not of a lack of expertise or precision on the part of the analyst.

The reduced effort associated with inverse analysis results from the fact that there is no need to reduce and plot the measured data in the form required for type-curve matching, the process of manually manipulating the data and type-curves is eliminated, and that it is not necessary to compute the formation parameters from the dimensionless results derived by type-curve matching. The inverse analysis approach does require that input data sets be configured prior to the analysis. This task requires knowledge of reasonable initial estimates and permissible ranges of values for the parameters that are to be determined in the analysis, appropriate values for the parameters that are to be assumed a priori, and the modelling scenario that is to be applied to the data. Thus, a significant level of understanding of the hydrogeology of the sampled formation is required, a requirement that mandates that inverse analysis be performed by a competent practitioner. Clearly, some preliminary, manual evaluation of the measured data is required to provide input to the automated analysis. In general, this preliminary effort may be performed with less precision than is required in the case where no further refinement of the estimates is possible. Thus, the use of preliminary results does not compromise the potential for the reduced analytical effort that is offered as an advantage of inverse analysis. The reduced effort associated with inverse analysis is most apparent in situations where a number of related sets of data are interpreted and a template input file can be configured; an example is the analysis of data assuming a range of modelling scenarios.

The reduced subjectivity associated with inverse analysis is a product of the automated manipulation of the calculated results. For given measured data and similar constraints on the analysis, the results extracted by two practitioners are likely to be equal. This is not the case for manual type-curve matching where different operators derive differing matches which translate to differing estimates of the parameters.

Importantly, the ability of the optimization algorithm to detect the optimal match between the measured data and calculated results yields higher resolution estimates of the parameters and provides for a meaningful comparison of the results achieved assuming a range of modelling scenarios. For example, in Figure 1, Cases 2 and 3 better represent the measured data than does Case 1 and therefore there is a rational basis for the prediction of a near-wellbore region of reduced transmissivity. In contrast, the discrepancy between the measured data and the manual match is such that it would be impossible to characterize the subtle influence of the near-wellbore conditions if the same resolution was achieved.

The method of inverse analysis described in this paper implements the TYPCURV and RADT models of fluid flow and tracer transport with minimal revisions to the source code. This use of existing models eliminates the development of redundant modelling capacity and assists in the timely development of an interpretive capability to accompany the formulation of new predictive models.

In conclusion, TCINV represents a useful tool for the analysis of hydraulic and tracer test data collected during in situ tests performed in fractured and porous media. This utility is realized despite the rather basic functionality entrained in TCINV. Recent progress in automated analysis of well-test data is described by Horne (1994). Additional features such as the determination of confidence intervals for the parameter estimates (Dogru et al., 1977), automated model configuration (Allain and Horne, 1990), and inversion of the data in Laplace space (Bourgeois and Horne, 1993) can be added to the algorithm as required.

Acknowledgements

The authors would like to thank Roland Horne of the Petroleum Engineering Department of Stanford University for his thoughtful contributions to the development of TCINV.

References

Allain, O.F., and Horne, R.N., 1990, Use of artificial intelligence in well-test interpretation: Journal of Petroleum Technology, Vol. 42, p. 342–349.

Bourgeois, M.J., and Horne, R.N., 1993, Well-test-model recognition with Laplace space: Society of Petroleum Engineers Journal of Formation Evaluation, Vol. 8, p. 17–25.

Carroll, J.A., III, and Horne, R.N., 1992, Multivariate optimization of production systems: Journal of Petroleum Technology, Vol. 44, p. 782–789.

Dogru, A.H., Dixon, T.N., and Edgar, T.F., 1977, Confidence limits on the parameters and predictions of slightly compressible, single-phase reservoirs: Society of Petroleum Engineers Journal, Vol. 263, p. 42–56.

Earlougher, R.C., Jr., 1977, Advances in Well Test Analysis: Society of Petroleum Engineers, New York, 264 p.

Gioda, G., and Maier, G., 1980, Direct search solution of an inverse problem in elastoplasticity: Identification of cohesion, friction angle and in situ stress by pressure tunnel tests: International Journal for Numerical Methods in Engineering, Vol. 15, p. 1823–1848.

Horne, R.N., 1990, Modern Well Test Analysis: Petroway, Palo Alto, 185 p.

Horne, R.N., 1994, Advances in computer-aided well-test interpretation: Journal of Petroleum Technology, Vol. 46, p. 599–606.

Nelder, J.A., and Mead, R., 1965, A simplex method for function minimization: Computer Journal, Vol. 7, p. 309–313.

Novakowski, K.S., 1988, Comparison of fracture aperture widths determined from hydraulic measurements and tracer experiments: Proceedings of the 4th Canadian/American Conference on Hydrogeology, National Water Well Association, Dublin, Ohio, p. 68–80.

Novakowski, K.S., 1990, Analysis of aquifer tests conducted in fractured rock: A review of the physical background and the design of a computer program for generating type curves: Ground Water, Vol. 28, p. 99–107.

Novakowski, K.S., 1992, The analysis of tracer experiments conducted in divergent radial flow fields: Water Resources Research, Vol. 28, p. 3215–3225.

Novakowski, K.S. and Lapcevic, P.A., 1994, Field measurement of radial solute transport in fractured rock: Water Resources Research, Vol. 30, p. 37–44.

Piggott, A.R., 1995, Automated analysis of hydraulic and tracer tests conducted in fractured rock: User's manual for TCINV: NWRI contribution number 95–29, 21 p.

Piggott, A.R., Brady, B.H., and Gu, H., 1992, Reservoir formation characterization from hydraulic fracturing records: Proceeding of Eurock '92, Thomas Telford, London, p. 360–365.

Piggott, A.R., and Elsworth, D., 1993, Characterization of fracture aperture by inverse analysis: Canadian Geotechnical Journal, Vol. 30, p. 637–646.

Piggott, A.R., Bobba, A.G., and Xiang, J., 1994, Inverse analysis implementation of the SUTRA groundwater model: Ground Water, Vol. 32, p. 829–836.

Piggott, A.R., and Novakowski, K.S., 1995, Determination of solution criteria for a semi-analytical model of solute transport: Computers and Geosciences, in press.

Rosa, A.J., and Horne, R.N., 1991, Automated well test analysis using robust (LAV) nonlinear parameter estimation: Proceedings of the 66th Annual Technical Conference and Exhibition of the Society of Petroleum Engineers, Vol. Ω, Society of Petroleum Engineers, Richardson, Texas, p. 191–206.

Press, W.H., Teukolsky, S.A., Vetterling, W.T., and Flannery, B.P., 1992, Numerical Recipes in FORTRAN: Cambridge University Press, Cambridge, 963 p.

Voss, C.I., 1984, A finite element simulation model for saturated-unsaturated, fluid density dependent groundwater flow with energy transport or chemically reactive single species solute transport: United States Geological Survey Water Resources Investigations Report 84–4369, 409 p.

Xiang, Y., Sykes, J.F., and Thomson, N.R., 1993, A composite L_1 parameter estimator for model fitting in groundwater flow and solute transport simulation: Water Resources Research, Vol. 29, p. 1661–1673.

Table 1. Parameters determined from the pulse test data				
Parameter	Manual	Case 1	Case 2	Case 3
T_2 (m^2/s)	6.2×10^{-6}	7.95×10^{-6}	1.05×10^{-5}	1.05×10^{-5}
S_2	8.0×10^{-7}	1.00×10^{-6}	2.64×10^{-7}	2.65×10^{-7}
S_{k2}			5.32×10^{0}	
r_s (m)				3.34×10^{-1}
T_1 (m^2/s)				3.05×10^{-6}
S_1				2.65×10^{-7}
Error	6.10×10^{-2}	1.33×10^{-2}	7.36×10^{-3}	7.36×10^{-3}

Table 2. Parameters determined from the pumping test data					
Parameter	Manual	Case 1	Case 2	Case 3	Case 4
T_2 (m^2/s)	7.0×10^{-6}	4.68×10^{-6}	4.65×10^{-6}	4.66×10^{-6}	4.73×10^{-6}
S_2	8.0×10^{-7}	1.95×10^{-6}	2.04×10^{-6}	2.02×10^{-6}	1.89×10^{-6}
S_{k1}					6.20×10^{0}
S_{k2}			-5.82×10^{0}		-5.52×10^{0}
r_s (m)				2.36×10^{-1}	
T_1 (m^2/s)				5.63×10^{-5}	
S_1				2.02×10^{-6}	
Error	8.23×10^{-2}	2.21×10^{-2}	1.98×10^{-2}	2.14×10^{-2}	1.99×10^{-2}

Table 3. Parameters determined from the tracer test data			
Parameter	Manual	Case 1	Case 2
b (m)	2.26×10^{-4}	1.77×10^{-4}	1.89×10^{-4}
α_r (m)	2.0×10^{-1}	3.04×10^{-1}	2.66×10^{-1}
θ_2	2.28×10^{-2}	1.76×10^{-2}	2.26×10^{-2}
r_i (m)			2.50×10^{1}
Error	1.09×10^{-3}	1.06×10^{-4}	8.47×10^{-5}

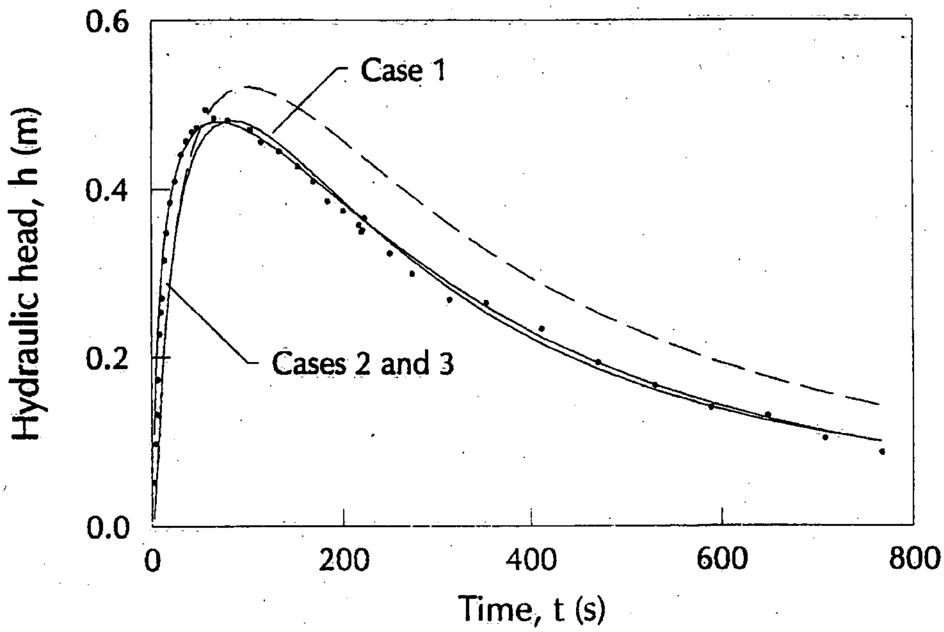

Figure 1. Measured data and calculated results for a pulse test conducted in fractured rock.

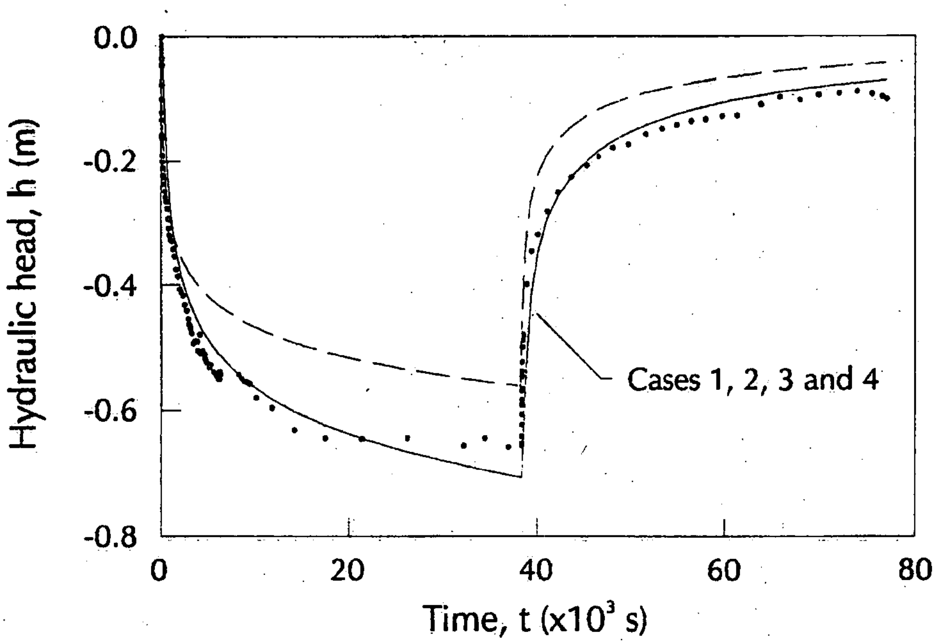

Figure 2. Measured data and calculated results for a pumping test conducted in fractured rock.

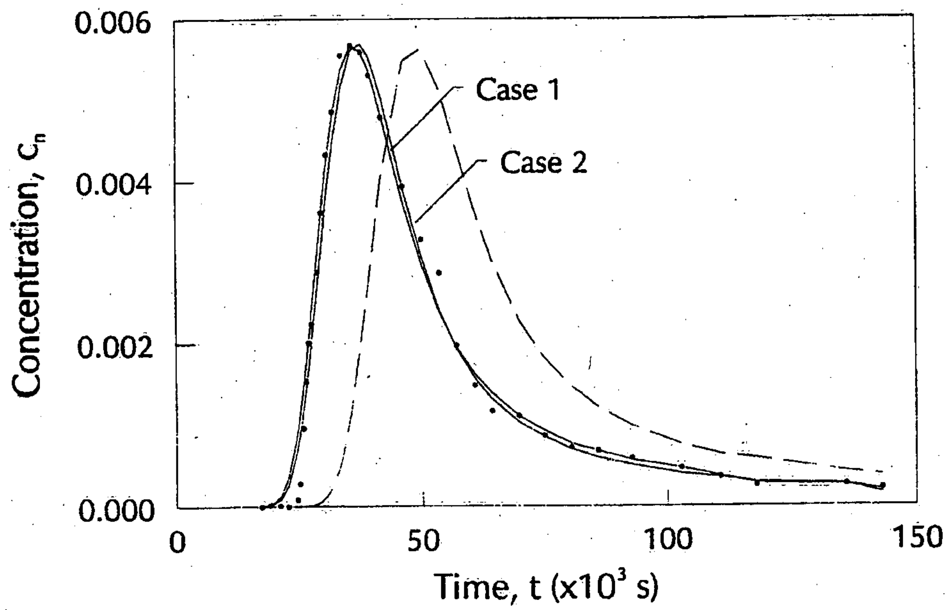

Figure 3. Measured data and calculated results for a tracer test conducted in fractured rock.

Canada Centre for Inland Waters
P.O. Box 5050
867 Lakeshore Road
Burlington, Ontario
L7R 4A6 Canada

National Hydrology Research Centre
11 Innovation Boulevard
Saskatoon, Saskatchewan
S7N 3H5 Canada

St. Lawrence Centre
105 McGill Street
Montreal, Quebec
H2Y 2E7 Canada

Place Vincent Massey
351 St. Joseph Boulevard
Gatineau, Quebec
K1A 0H3 Canada

Centre canadien des eaux intérieures
Case postale 5050
867, chemin Lakeshore
Burlington (Ontario)
L7R 4A6 Canada

Centre national de recherche en hydrologie
11, boul. Innovation
Saskatoon (Saskatchewan)
S7N 3H5 Canada

Centre Saint-Laurent
105, rue McGill
Montréal (Québec)
H2Y 2E7 Canada

Place Vincent-Massey
351 boul. St-Joseph
Gatineau (Québec)
K1A 0H3 Canada